# Supplement for "Functional Alignment with Anatomical Networks is Associated with Cognitive Flexibility"

John D. Medaglia[1,2], Weiyu Huang[3], Elisabeth A. Karuza[4], Apoorva Kelkar[1], Sharon L. Thompson-Schill[4], Alejandro Ribeiro[3], and Danielle S. Bassett[3,5]

[1] *Department of Psychology, Drexel University, Philadelphia, PA, 19104 USA*
[2] *Department of Neurology, Perelman School of Medicine, University of Pennsylvania, Philadelphia, PA, 19104 USA*
[3] *Department of Electrical & Systems Engineering, University of Pennsylvania, Philadelphia, PA, 19104 USA*
[4] *Department of Psychology, University of Pennsylvania, Philadelphia, PA, 19104 USA*
[5] *Department of Bioengineering, University of Pennsylvania, Philadelphia, PA, 19104 USA*

# Supplementary Results

## Behavior

Across the 28 subjects, individuals were 94% (St.D. = 1%) accurate across all trials. The average median response time for accurate non-switching trials was 0.89 s (St.D. = 0.12 s). The average median response time for accurate switching trials across subjects was 1.22 s (St.D. = 0.18 s). The average switch cost across subjects was 0.32 s (St.D. = 0.08 s).

## The concentration of aligned and liberal signals is observed in specific regions

As we note in the methods, our application of the GFT can identify the extent to which individual nodes contribute to both aligned and liberal signals, and these quantities are not mutually exclusive. In the main text, we note that the insula, anterior cingulate, and subcortical systems share both aligned and liberal signals. We quantified the relationship between aligned and liberal signals by calculating the Pearson correlation coefficient between alignment and liberality values over all brain regions. We observed that the two types of signals were significantly but not perfectly correlated across the brain (mean over subjects and tasks $R = 0.69, p \ll 0.001$). This analysis highlights an interesting measure of multimodal complexity that differs across brain areas: subcortical regions can be thought of as displaying high multimodal complexity because they contain both highly anatomically-aligned signals and highly anatomically-liberal signals.

## Signal alignment stability in human brain networks

We asked whether the observed regional variation in aligned and liberal signals could be estimated reliably across subjects and tasks, supporting its utility as a stable marker for switching behavior. To examine the stability of aligned and liberal signals across all individual conditions, we compute a Pearson's correlation coefficient between the signal concentration vector across regions for each condition pair among aligned and liberal signal vectors for the fixation, no switch, and switching blocks. We observe that the aligned and liberal signals are very highly stable for each pairwise correlation within each signal type, but only moderately correlated across signal types (within aligned: mean $R = 0.99, p \ll 0.001$, within liberal: mean $R = 0.99, p \ll 0.001$, between aligned and liberal: mean $R = 0.69, p \ll 0.001$; See. Fig. 1). These results establish that during periods of resting fixation, no switching demands, and switching demands in the Navon task, alignment and liberality are highly stable subject-level traits.

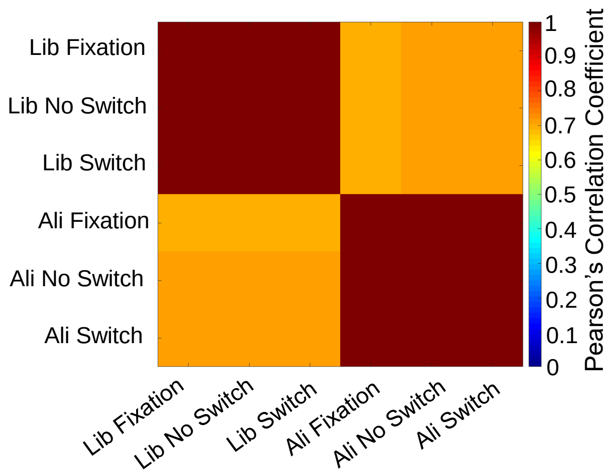


Supplementary Figure 1: **Aligned and liberal signals are consistent traits in human brain networks.** Correlations among conditions decomposing BOLD fMRI signals using the eigenspectrum of the 28 individuals' anatomical networks. Aligned and liberal signals are highly stable at the subject level. Ali = aligned, Lib = liberal.

## Signal variability in systems

In the main text, we note that signals that are highly aligned with the underlying anatomical networks were concentrated in fronto-parietal, cingulo-opercular, default mode, and subcortical systems. This is especially interesting given numerous findings identifying the fronto-parietal and cingulo-opercular systems to contain variable signals over time and more flexible changes in network organization during both rest and task performance [1, 2]. To examine the BOLD signal variability in systems across TRs in the current study, we compute the average standard deviation of BOLD time series values over trials for all regions within each system. Then, we conduct a non-parametric permutation test in which we shuffle the assignment of regions to systems ($n = 10,000$) and compute a null distribution of average time series standard deviations over TRs for each system. We judge a system to be significantly variable or invariant over time if its observed average standard deviation is greater than or less than 97.5% of null permutations. We find that the fronto-parietal and cingulo-opercular systems are more variable across TRs than the null expectation, whereas the ventral attention, somatosensory, and cerebellar systems are less variable. Considered together with our main results examining aligned and liberal signal concentrations, these results indicate that in cognitive control systems that are functionally dynamic, signal variance is strongly organized by aligning with subject's anatomical networks from TR to TR.

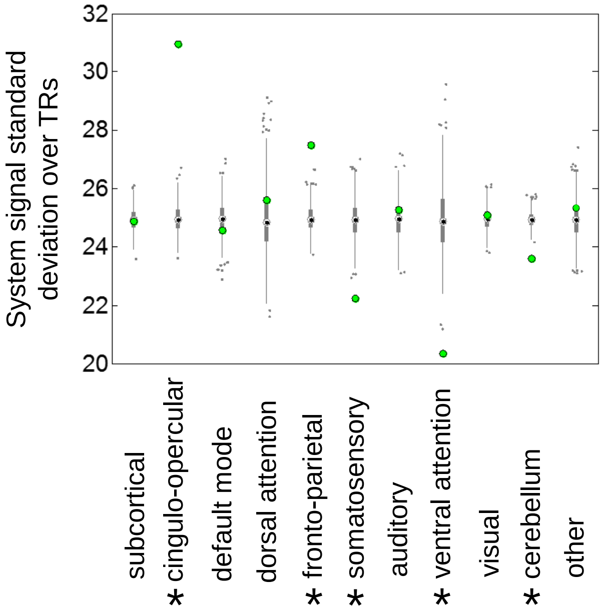


Supplementary Figure 2: **System-level variability across TRs.** Plot of system-level variability in BOLD time series across TRs for the 28 subjects. Boxes and whiskers illustrate the distribution of system average standard deviation of BOLD time series over TRs for each system. Green circles illustrate the observed average standard deviations across TRs in each system. Asterisks denote systems in which the observed means were higher or lower than 97.5% of permuted values.

## System flexibility is associated with signal alignment

In the main manuscript, we focus on the trial-to-trial signal alignment with anatomy across the brain as a basic spatiotemporal unity contributing to brain signal organization. We remark that previous analyses have focused on a notion of "flexibility" in dynamic networks. This notion is represented by creating a three-dimensional tensor from consecutive or overlapping association matrices (e.g., using correlation, coherence, or mutual information) and observing the changes in node community allegiance over time. Flexible nodes are those that exhibit a relatively high degree of changes in community assignments. Distinct from the current analysis, flexibility occurs at a longer temporal scale since tensors are constructed from many adjacency matrices over time, which in turn are computed over many TRs of time series data. In this context, it is interesting to consider whether the anatomical alignment of BOLD signals at the TR level is associated with the expression of flexibility at the temporal network level.

To explore the relationship between flexible systems and signal alignment with anatomy, we explicitly computed flexibility and associated these values within each subjects's alignment values. Specifically, we followed [3] to examine the dynamic community structure of the current data. We constructed a multilayer temporal network for each subject by computing the correlation between all region pairs. Correlations whose significance did not pass false discovery rate correction with a threshold of 0.05 were set to zero [4] for each of 10 non-overlapping windows (40 TRs apiece) over the entire task session. We maximized multilayer modularity $Q_{ml}$ following [5]:

$$Q_{ml} = \frac{1}{2\mu} \sum_{ijlr} \left\{ \left( A_{ijl} - \gamma_l \frac{k_{il} k_{jl}}{2m_l} \right) \delta_{lr} + \delta_{ij} C_{jlr} \right\} \delta(g_{il}, g_{jr}),$$

where the adjacency matrix of layer $l$ (i.e., time window number $l$) has components $A_{ill}$, $\gamma_l$ is the resolution parameter of layer $l$, $g_{il}$ gives the community assignment of node $i$ in layer $l$, $g_{jr}$ gives the community assignment of node $j$ in layer $r$, $C_{jlr}$ is the connection strength between node $j$ in layer $r$ and node $j$ in layer $l$ (see the discussion below), $k_{il}$ is the strength of node $i$ in layer $l$, $2\mu = \sum_{jr} k_{jr}, k_{jl} = k_{jl} + c_{jl}$, and $c_{jl} = \sum_r C_{jlr}$. For simplicity, we set the resolution parameter $\gamma_l$ to unity and we have set all non-zero $C_{jlr}$ to a constant $C$, which we term the inter-layer coupling. Here, we compute community assignments for $C = 1$. For each subject, we optimized the quality function 100 times and identified a representative consensus partition for all nodes over all windows [6].

Within each subject's consensus partition, we defined the flexibility of a node $f_i$ to be the number of times that node changed modular assignment throughout the session, normalized by the total number of changes that were possible (i.e., by the number of consecutive pairs of layers in the multilayer framework) [4]. We then defined the flexibility of each system examined in the main text as the mean flexibility over all nodes in the subsystem. Finally, we calculated the Pearson correlation coefficient between the mean system flexibility and mean system alignment. Notably, we found that mean flexibility and mean alignment were significantly positively correlated with one another across systems ($R = 0.15, p = 0.015$). This result indicates that trial-level signal alignment across the brain is positively associated with the expression of temporal system flexibility over much larger temporal scales across brain networks.

# Signal alignment in anatomy is similar to function

To provide further intuition for our observation that signal alignment is greatest in the most flexible systems, we highlight that the seemingly counterintuitive observation – the regions whose signals are aligned with the underlying structural network are also the regions that display the greatest network flexibility across time points – is mathematically justifiable. The reason comes from the close relationship between the graph Fourier transform (GFT) and Principal Component Analysis (PCA) [7, 8], when the network represents pairwise correlations between brain regions across time points. In this case, from PCA, the signal distribution that explains most of the variation of signals across time points is represented by the eigenvectors associated with large eigenvalues of the correlation matrix (functional connectivity network). Simultaneously, recall from GFT that the eigenvectors associated with large eigenvalues of the correlation matrix depict signal distributions that align well with the network [9, 10]. This implies that the signal distribution that aligns with the network representing pairwise correlations between brain regions also varies the most across time points. Stated simply, it can be derived mathematically that the most flexible systems are most aligned with the functional network constructed from those signals [11].

Thus, crucial to the current result, if the correlation matrix's eigenspectrum is similar to the anatomical network, the most anatomically aligned functional signals will also be related to the most functionally aligned and flexible signals. In order to evaluate this relationship empirically, we examined the correlation between signals aligned with the structural networks and signals aligned with the functional networks. For each subject in the experiment, we constructed the subject's correlation matrix across all TRs and performed the same decomposition of each BOLD TR from our primary analysis using each subject's (1) anatomical network and then repeated this analysis using (2) the correlation matrix across all BOLD TRs. Next, we examined the similarity between the signals aligned with the functional correlation network and those aligned with the anatomical network. A significant correlation would indicate that the decomposition of the aligned portion of signals is organized with the functional correlation network similarly to its decomposition into the anatomical network, suggesting that the relationships between flexibility and alignment is expressed both in the subject's anatomical and mean functional correlation network.

We find a strong correlation between the anatomically and functionally aligned signals ($R = 0.814$, $p = 1.613 \times 10^{-27}$). This empirical relationship indicates that signals most aligned with the functional network are those most aligned with the anatomical network. Thus, the eigenspectrum of the functional network that contributes to the tendency for flexible functional signals to align is related to the anatomical eigenspectrum across subjects. This highlights a fundamental relationship guiding BOLD signal dynamics in anatomical and functional network analysis. Both anatomical and functional correlation networks demonstrate an eigenspectrum that organizes flexible activity in the human brain.

## Aligned and liberal signal associations with Navon task behavior across task conditions

In the main text, we focus on the relationship between variability in signal alignment and variability in switch costs due to our emphasis on cognitive control − and in particular, cognitive flexibility − in human brain networks. For reference, here we include a full table of results associating median response times in each condition (no switching, switching, and switch costs) with aligned and liberal signals across the 28 subjects. The results indicate that within the current signal decomposition using anatomical networks, only the liberal signals demonstrate a relationship with behavioral variability and specifically with switch costs. Moreover, given consistently significant correlations between BOLD signal liberality in each block type and Navon switching performance, we conducted *post hoc* partial correlations to test whether unique block-level relationships existed. To do so, we computed the partial correlation between BOLD signal liberality for each block type (fixation, non-switching blocks, and switching blocks) and Navon switch costs covarying for the signal in the other two block types and motion. No correlations survive ($p >> 0.05$ for all combinations). This indicates that BOLD signal liberality exhibits a stable relationship with overall switch costs across the time series.

Supplementary Table 1: **Pearson's partial correlation coefficients for all median response time associations with signal liberality and alignment.**

| Behavior | Lib Fix | Lib NS | Lib S | Ali Fix | Ali NS | Ali S |
|---|---|---|---|---|---|---|
| No Switch | 0.2223 | 0.3503 | 0.2207 | 0.0328 | 0.1134 | -0.0907 |
| Switch | 0.4264 | 0.5563 | 0.4026 | 0.1962 | 0.2298 | 0.0090 |
| Switch Cost | 0.6181 | 0.7137 | 0.5669 | 0.3912 | 0.3431 | 0.1599 |

Pearson's correlation coefficients using average framewise displacement as a covariate. Rows contain partial correlation coefficients associating each median response time at the subject level with their graph alignment. Columns represent the signal type including the fixation, no switch, and switch block signals. Lib = liberal, Ali = aligned, Fix = fixation, NS = no switch, S = switch.

Supplementary Table 2: **Pearson's partial correlation $p$-values: all median response time associations with signal liberality and alignment.**

| Behavior | Lib Fix | Lib NS | Lib S | Ali Fix | Ali NS | Ali S |
|---|---|---|---|---|---|---|
| No Switch | 0.2650 | 0.0733 | 0.2686 | 0.8709 | 0.5734 | 0.6526 |
| Switch | 0.0266 | 0.0026 | 0.0374 | 0.3267 | 0.2488 | 0.9644 |
| Switch Cost | 0.0006 | <0.0001 | 0.0020 | 0.0436 | 0.0798 | 0.4258 |

Rows contain $p$-values corresponding to correlation coefficients in Table 1. Columns represent the signal type including the fixation, no switch, and switch block signals. Lib = liberal, Ali = aligned, Fix = fixation, NS = no switch, S = switch.

## Inclusion of age and sex as covariates in the Navon task analysis

In the main text, we relate alignment and liberality to behavior using subjects' average framewise displacement as covariates. To examine whether our results are stable when accounting for subjects' age and sex, we recompute partial correlations for each task condition and alignment and liberality values using average framewise displacement, age, and sex as covariates. Our results remain significant with similar correlation values across conditions when including these covariates, indicating that the relationship between liberality and cognitive switching performance is not influenced by these variables.

Supplementary Table 3: **Pearson's partial correlation coefficients for all median response time associations with signal liberality and alignment.**

| Behavior | Lib Fix | Lib NS | Lib S | Ali Fix | Ali NS | Ali S |
|---|---|---|---|---|---|---|
| No Switch | 0.3508 | 0.4990 | 0.4116 | 0.1168 | 0.1842 | -0.0042 |
| Switch | 0.5009 | 0.6443 | 0.5390 | 0.2319 | 0.2390 | 0.0527 |
| Switch Cost | 0.6028 | 0.7052 | 0.5984 | 0.3459 | 0.2629 | 0.1237 |

Pearson's correlation coefficients using average framewise displacement, age, and sex as covariates. Rows contain partial correlation coefficients associating each median response time at the subject level with their graph liberality. Columns represent the signal type including the fixation, no switch, and switch block signals. Lib = liberal, Ali = aligned, Fix = fixation, NS = no switch, S = switch.

Supplementary Table 4: **Pearson's partial correlation $p$-values: all median response time associations with signal liberality and alignment.**

| Behavior | Lib Fix | Lib NS | Lib S | Ali Fix | Ali NS | Ali S |
|---|---|---|---|---|---|---|
| No Switch | 0.0856 | 0.0111 | 0.0409 | 0.5783 | 0.3780 | 0.9842 |
| Switch | 0.0107 | 0.0005 | 0.0054 | 0.2646 | 0.2499 | 0.8023 |
| Switch Cost | 0.0014 | 0.0001 | 0.0016 | 0.0903 | 0.2042 | 0.5559 |

Rows contain $p$-values corresponding to correlation coefficients in Table. Columns represent the signal type including the fixation, no switch, and switch block signals. Lib = liberal, Ali = aligned, Fix = fixation, NS = no switch, S = switch.

## Testing whether the relationship between BOLD signal alignment and Navon task performance is similar across task conditions.

While we find consistent significant relationships between BOLD signal liberality and Navon switching costs across all portions of the task in our primary analysis, it is critical to test whether the relationship between the brain and behavioral measures are uniquely high in any portion of the task. In combination with our analyses demonstrating that the alignment values are highly stable across task blocks (see "Signal alignment as a trait-level variable in human brain networks, above"), this helps to establish whether the BOLD signal alignment is more like a trait versus a state variable in predicting cognitive flexibility. To test this possibility, we computed partial correlations associating signal alignment values in each block with the Navon performance variables covarying for the signal alignment values in the other blocks. These analyses reveal that the relationship between signal alignment and Navon performance in each block falls below statistical significance when covarying for alignment values in other blocks. Considered together with the stability of liberality across blocks, this suggests that signal liberality is a stable property associated with cognitive flexibility under a switching task set.

Supplementary Table 5: **Pearson's partial correlation coefficients for Navon task performance using BOLD signal alignments from the two other block types as covariates.**

| Behavior | Lib Fix | Lib NS | Lib S | Ali Fix | Ali NS | Ali S |
|---|---|---|---|---|---|---|
| No Switch | -0.0232 | 0.2355 | -0.0843 | 0.0223 | 0.1297 | -0.1586 |
| Switch | 0.0442 | 0.3086 | -0.0477 | 0.1225 | 0.1361 | -0.1464 |
| Switch Cost | 0.1637 | 0.3601 | 0.0418 | 0.2483 | 0.1088 | -0.0849 |

Pearson's correlation coefficients in Switching tasks using average framewise displacement and average signals from the other two block types as covariates. Rows contain partial correlation coefficients associating each median response time at the subject level with their graph liberality. Columns represent the signal type including the fixation, no switch, and switch block signals. Lib = liberal, Ali = aligned, Fix = fixation, NS = no switch, S = switch. As an example, the entry in the first column first row indicates the correlation coefficient between liberal signal from Fix signal blocks and no switch median RT, using liberal signal from S and NS signal blocks as covariates.

Supplementary Table 6: **Pearson's partial correlation $p$-values for the relationship between Navon task performance and BOLD signal alignment using signals from the other two blocks as covariates.**

| Behavior | Lib Fix | Lib NS | Lib S | Ali Fix | Ali NS | Ali S |
|---|---|---|---|---|---|---|
| No Switch | 0.9124 | 0.2570 | 0.6888 | 0.9156 | 0.5365 | 0.4489 |
| Switch | 0.8340 | 0.1333 | 0.8209 | 0.5596 | 0.5165 | 0.4850 |
| Switch Cost | 0.4343 | 0.0771 | 0.8428 | 0.2315 | 0.6048 | 0.6867 |

Rows contain $p$-values corresponding to correlation coefficients in Table 5. Columns represent the signal type including the fixation, no switch, and switch block signals. Lib = liberal, Ali = aligned, Fix = fixation, NS = no switch, S = switch.

## Aligned and liberal signal associations with Navon task performance controlling for non-switching performance

In the main text, we focus on the relationship between variability in signal alignment and variability in switch costs due to our emphasis on cognitive control in human brain networks. For reference, here we include results associating median response times in the switch cost condition with aligned and liberal signals across the 28 subjects. The results indicate that within the current signal decomposition using anatomical networks, the liberal signals demonstrate a relationship with switch costs above and beyond non-switching performance.

Supplementary Table 7: **Pearson's partial correlation coefficients for all Navon task median response time associations between signal liberality and alignment using non-switching performance as a covariate.**

| Behavior | Lib Fix | Lib NS | Lib S | Ali Fix | Ali NS | Ali S |
|---|---|---|---|---|---|---|
| Switch Cost | 0.6181 | 0.7137 | 0.5669 | 0.3912 | 0.3431 | 0.1599 |

Pearson's partial correlation coefficients using average framewise displacement as a covariate. Columns represent the signal type including the fixation, no switch, and switch block signals. Lib = liberal, Ali = aligned, Fix = fixation, NS = no switch, S = switch.

Supplementary Table 8: **Pearson's partial correlation $p$-values for all Navon task median response time associations between signal liberality and alignment using non-switching performance as a covariate.**

| Behavior | Lib Fix | Lib NS | Lib S | Ali Fix | Ali NS | Ali S |
|---|---|---|---|---|---|---|
| Switch Cost | 0.0006 | <0.0001 | 0.0020 | 0.0436 | 0.0798 | 0.4258 |

Rows contain $p$-values corresponding to correlation coefficients in Table 1. Columns represent the signal type including the fixation, no switch, and switch block signals. Lib = liberal, Ali = aligned, Fix = fixation, NS = no switch, S = switch.

## Liberal signal associations with Navon task performance controlling for aligned signals

While no significant correlation was observed between Navon task performance and aligned signals, it is possible that shared variance between aligned and liberal signals may relate to performance. To test this possibility, we computed the partial correlation between BOLD signal liberality and Navon task performance. This reveals that the associations between Navon task performance and liberality remain significant above and beyond BOLD signal alignment.

Supplementary Table 9: **Pearson's partial correlation coefficients for all Navon task median response time associations with signal liberality using signal alignment as a covariate.**

| Behavior | Lib Fix | Lib NS | Lib S |
|---|---|---|---|
| No Switch | 0.2387 | 0.2549 | 0.1988 |
| Switch | 0.3892 | 0.4403 | 0.3712 |
| Switch Cost | 0.5352 | 0.6125 | 0.5386 |

Pearson's correlation coefficients for the association between liberality and Navon task performance using average framewise displacement and alignment as covariates. Rows contain partial correlation coefficients associating each median response time at the subject level with their graph liberality. Columns represent the signal type including the fixation, no switch, and switch block signals. Lib = liberal, Fix = fixation, NS = no switch, S = switch.

Supplementary Table 10: **Pearson's partial correlation $p$-values for all Navon task median response time associations with signal liberality using signal alignment as a covariate**

| Behavior | Lib Fix | Lib NS | Lib S |
|---|---|---|---|
| No Switch | 0.2403 | 0.2089 | 0.3304 |
| Switch | 0.0494 | 0.0244 | 0.0619 |
| Switch Cost | 0.0048 | 0.0009 | 0.0045 |

Rows contain $p$-values corresponding to correlation coefficients in Table 9. Columns represent the signal type including the fixation, no switch, and switch block signals. Lib = liberal, Fix = fixation, NS = no switch, S = switch.

## Contribution of the cerebellum in associations between signals with and without the cerebellum during the Navon task

In the main text, all analyses report results based on cortical, subcortical, and cerebellar regions. Notably, we excluded intracerebellar connections as likely spurious connections due to a known lack of direct anatomical lobule-to-lobule connections in the cerebellum. We also observed that the cerebellum contributed the lowest amount of aligned and liberal signals in the brain, suggesting that it does not contribute substantially to our behavioral results. To examine this possibility explicitly, we repeated our partial correlation analyses associating aligned and liberal signals observed in the 83 cortical and cortical regions not including the cerebellum using average framewise displacement as a covariate. The resulting correlations between liberality and switching and switch cost performance remain statistically significant for all block types, suggesting that the switching-relevant signals are robustly observed in non-cerebellar regions.

Supplementary Table 11: **Pearson's partial correlation coefficients for all Navon median response time associations with signal liberality and alignment without the cerebellum**

| Behavior | Lib Fix | Lib NS | Lib S | Ali Fix | Ali NS | Ali S |
|---|---|---|---|---|---|---|
| No Switch | 0.2462 | 0.3706 | 0.3015 | 0.1170 | 0.1964 | 0.0086 |
| Switch | 0.4156 | 0.5360 | 0.4607 | 0.2336 | 0.2514 | 0.0659 |
| Switch Cost | 0.5658 | 0.6519 | 0.5852 | 0.3493 | 0.2725 | 0.1343 |

Pearson's correlation coefficients using average framewise displacement, age, and sex as covariates, without the cerebellum. Rows contain partial correlation coefficients associating each median response time at the subject level with their graph alignment or liberality. Columns represent the signal type including the fixation, no switch, and switch block signals. Lib = liberal, Ali = aligned, Fix = fixation, NS = no switch, S = switch.

Supplementary Table 12: **Pearson's partial correlation *p*-values for all Navon median response time associations with signal liberality and alignment without las 28 regions.**

| Behavior | Lib Fix | Lib NS | Lib S | Ali Fix | Ali NS | Ali S |
|---|---|---|---|---|---|---|
| No Switch | 0.2355 | 0.0682 | 0.1430 | 0.5776 | 0.3467 | 0.9676 |
| Switch | 0.0388 | 0.0057 | 0.0205 | 0.2611 | 0.2255 | 0.7544 |
| Switch Cost | 0.0032 | 0.0004 | 0.0021 | 0.0870 | 0.1875 | 0.5221 |

Rows contain *p*-values corresponding to correlation coefficients in Table 11. Columns represent the signal type including the fixation, no switch, and switch block signals. Lib = liberal, Ali = aligned, Fix = fixation, NS = no switch, S = switch.

## Aligned and liberal signal associations with Stroop and n-back task behavior across task conditions

We maintain a theoretical interest in flexibility represented by switching in the primary text, but cognitive switching is only one of several so-called "cognitive control" functions. Cognitive inhibition and working memory are also often examined in cognitive control research [12]. Indeed, cognitive inhibition may be involved in the Navon task examined here because individuals must inhibit the tendency to respond according to the opposite rule during each trial, with an extra inhibition demand on the switching trials [13, 14, 15]. Working memory demands during the Navon and Stroop may be relatively low because stimuli remain clearly visible on the screen during each trial, but working memory may also be involved to maintain rule set [16]. Thus, to establish whether signal alignment is not only sensitive but specific to cognitive switching, examining alignment-behavior relationships during other tasks is necessary.

To examine the relationship between signal alignment and inhibition and working memory, we repeated our analyses in data collected during two additional tasks: a Stroop inhibition task and an n-back task. The Stroop inhibition task was collected during the same day of scanning as the Navon task in all 28 subjects included in the primary manuscript. This task acquired within-subjects allowed us to examine cognitive switching performance while accounting for the variance in (1) inhibition performance and (2) BOLD signal alignment and liberality during the Stroop task. Together, partial correlations including these as covariates in the Navon analysis allow us to determine if the liberality-switching relationship in our primary results can be partially or fully attributable to Stroop inhibition demands or signal organization observed across both tasks. To examine working memory relationships with BOLD signal alignment and liberality, we selected the n-back task from 39 subjects (mean age 29.7 years (St. D. 3.7 years) [1]; 21 females) in the publicly available data in the Human Connectome Project [17]. We also examined resting state fMRI data from the Human Connectome Project to examine for relationships between resting signal alignment and working memory performance. We briefly describe the Stroop and n-back tasks here; see the Human Connectome Project primary documentation for further details on data collection procedures. All Stroop and n-back data were processed with an identical pipeline to the data collected for the Navon task. Resting data were processed with a pipeline validated for superior performance in removing motion artifacts (a 36-parameter nuisance regression model with despiking [18]; code available at https://github.com/PennBBL/xcpEngine). We used our average motion value as a covariate for all correlations between resting BOLD signal alignment and liberality as an additional protection against spurious findings due to motion artifacts.

### Stroop task.

The Stroop task was acquired in a comparable manner to the Navon task for each subject. All subjects completed a task based on the classic Stroop color-word paradigm [19] that involves a mismatch between a color word and the color it is printed in: for example, the word "red" printed in the color blue. The mismatch introduces an interference effect indicated by slower performance on trials with a color mismatch relative to those where the colors match or the word is not a color word. On all trials, stimuli comprised words printed in color on a gray background. There were two block types. The trials in the first block type included "neutral" [20] non-color words ("far", "deal", "horse", and "plenty") printed in red, green, yellow, or blue. In the second block type, the "response-eligible conflict trials presented color words ("red", "green", "yellow", and "blue") printed in a mismatching color: red, green, yellow or blue [20]. In all blocks, subjects were instructed to respond to the color the word was printed in, not what it explicitly states. Blocks were administered in a random order. Subjects responded using their right hand with a four-button box. All subjects were trained on the task outside the scanner until proficient at reporting responses using a fixed finger mapping between the shape and the button presses (i.e., index finger = "red", middle finger = "green", ring finger = "yellow", and pinky finger = "blue"). In the scanner, blocks were administered with 20 trials separated by 20 s fixation periods with a black crosshair at the center of the screen. Each trial was presented for a fixed duration of 1900 ms separated by an interstimulus interval of 100 ms during which a gray screen was presented. We computed the "interference effect" as the speed of accurate responses during the response-eligible conflict trials minus the neutral trials. This represents the "inhibition cost" presumed to operate when inhibiting the prepotent response to say the color word rather than the color it is printed in [21].

### n-Back task.

The n-back task is a classic working memory paradigm in which subjects must respond to trials based on whether the current trial matches that seen "n-back" ago. For example, a subject might observe one letter

[1] note that the HCP publicly available release only provides ages in 3-years intervals; we provide the average age across subjects based on the mean of the age bins provided in the HCP release for each subject

at a time on a computer screen. A “0-back” would require subjects to respond with a button press if the current stimulus matches one instructed *a priori* (such as an “X”), whereas a “2-back” would require subjects to respond with a button press if the current stimulus matches that two trials back. The difference in performance between the 2-back and the 0-back are thought to represent the working memory and control demands required to respond appropriately [22]. The Human Connectome Project used an n-back paradigm involving several different types of stimuli: body, faces, places, and tools administered in a mixed blocked and event-related design. A 2-second cue indicated the task type (and target for the 0-back) at the start of the block. Each of the two runs contained 8 task blocks (10 trials of 2.5 s each, for 25 seconds) and 4 fixation blocks (15 s). On each trial, the stimulus was presented for 2 s, followed by a 500 ms inter-trial interval.

The category specific representation task and the working memory task are combined into a single task paradigm. Participants were presented with blocks of trials that consisted of pictures of places, tools, faces and body parts (non-mutilated parts of bodies with no nudity). Within each run, the 4 different stimulus types were presented in separate blocks. Also, within each run, of the blocks use a 2-back working memory task and use a 0-back working memory task (as a working memory comparison). A 2.5 second cue indicates the task type (and target for 0-back) at the start of the block. Each of the two runs contains 8 task blocks (10 trials of 2.5 seconds each, for 25 seconds) and 4 fixation blocks (15 seconds). On each trial, the stimulus is presented for 2 seconds, followed by a 500 ms inter-task interval (ITI). HCP n-back data were acquired in both left-to-right and right-to-left phase encoding directions; we replicate our analysis in both datasets. All data were acquired with 720 ms TRs and 2mm isotropic voxels.

## Resting state data.

Finally, in the primary manuscript, we observed that signal alignment during the non-task fixation periods was significantly related to switch costs, suggesting that signal alignment may operate more like a trait than a state. We examined this same relationship in the Stroop inhibition task fixation periods within the Stroop to predict Stroop performance. We also examined whether BOLD signal liberality during the Stroop fixation was related to Navon performance, which allows us to test the notion that liberality is like a trait that exists across tasks that supports cognitive flexibility. To examine the relationship between “pure” resting state data and behavior, we computed signal alignment available in the Human Connectome Project resting state data and related it to performance observed on the n-back task. HCP resting data were acquired in both left-to-right and right-to-left phase encoding directions; we replicate our analysis in both datasets. All data were acquired with 720 ms TRs and 2mm isotropic voxels.

## Aligned and liberal signal associations with Stroop task behavior across task conditions.

Prior to using Stroop behavioral values as covariates in our analyses relating BOLD signal alignment with Navon performance, we include a full table of results associating median response times in each condition of the Stroop task (neutral trials, response-eligible, and inhibition costs) with aligned and liberal signals across the 28 subjects. The results indicate that within the current signal decomposition using anatomical networks, neither the aligned nor the liberal signals from any task block were significantly correlated with any Stroop performance measure.

Supplementary Table 13: **Pearson’s partial correlation coefficients for all Stroop median response time associations with signal liberality and alignment.**

| Behavior | Lib Fix | Lib N | Lib RE | Ali Fix | Ali N | Ali RE |
|---|---|---|---|---|---|---|
| Neutral | 0.0616 | 0.0472 | 0.2031 | -0.1497 | -0.1854 | -0.0876 |
| Response-eligible | 0.1059 | 0.0386 | 0.2028 | -0.0877 | -0.1819 | -0.0246 |
| Inhibition Cost | 0.1048 | -0.0115 | 0.0301 | 0.1112 | -0.0206 | 0.1228 |

Pearson’s correlation coefficients between BOLD signal alignment and liberality during the Stroop task and behavior using average framewise displacement as a covariate. Rows contain partial correlation coefficients associating each median response time at the subject level with their graph alignment. Columns represent the signal type including the fixation, neutral, and response-eligible block signals. Lib = liberal, Ali = aligned, Fix = fixation, N = neutral, RE = response-eligible.

Supplementary Table 14: **Pearson's partial correlation $p$-values for all Stroop median response time associations with signal liberality and alignment.**

| Behavior | Lib Fix | Lib N | Lib RE | Ali Fix | Ali N | Ali RE |
|---|---|---|---|---|---|---|
| Neutral | 0.7601 | 0.8150 | 0.3097 | 0.4561 | 0.3545 | 0.6639 |
| Response-eligible | 0.5992 | 0.8485 | 0.3103 | 0.6636 | 0.3637 | 0.9031 |
| Inhibition Cost | 0.6028 | 0.9544 | 0.8813 | 0.5807 | 0.9188 | 0.5417 |

Rows contain $p$-values corresponding to correlation coefficients in Table 13. Columns represent the signal type including the fixation, neutral, and response-eligible block signals. Lib = liberal, Ali = aligned, Fix = fixation, N = neutral, RE = response-eligible.

## Inclusion of age and sex as covariates in the Stroop task analysis.

For symmetry with our analyses in the Navon task subjects' age and sex, we recompute partial correlations for each Stroop task condition and alignment and liberality values using average framewise displacement, age, and sex as covariates. The relationships between BOLD signal alignment and Stroop performance remain insignificant with similar correlation values across conditions when including the covariates.

Supplementary Table 15: **Pearson's partial correlation coefficients for all Stroop median response time associations with signal liberality and alignment.**

| Behavior | Lib Fix | Lib N | Lib RE | Ali Fix | Ali N | Ali RE |
|---|---|---|---|---|---|---|
| Neutral | 0.0688 | 0.1021 | 0.2179 | -0.1227 | -0.1786 | -0.0540 |
| Response-eligible | 0.1039 | 0.0753 | 0.2061 | -0.0667 | -0.1962 | 0.0061 |
| Inhibition Cost | 0.0848 | -0.0422 | 0.0067 | 0.1016 | -0.0635 | 0.1202 |

Pearson's correlation coefficients between BOLD signal alignment and liberality during the Stroop task and behavior using average framewise displacement, age, and sex as covariates. Rows contain partial correlation coefficients associating each median response time at the subject level with their graph alignment or liberality. Columns represent the signal type including the fixation, neutral, and response-eligible block signals. Lib = liberal, Ali = aligned, Fix = fixation, N = neutral, RE = response-eligible.

Supplementary Table 16: **Pearson's partial correlation $p$-values for all Stroop median response time associations with signal liberality and alignment.**

| Behavior | Lib Fix | Lib N | Lib RE | Ali Fix | Ali N | Ali RE |
|---|---|---|---|---|---|---|
| Neutral | 0.7439 | 0.6271 | 0.2954 | 0.5589 | 0.3931 | 0.7976 |
| Response-eligible | 0.6212 | 0.7205 | 0.3229 | 0.7515 | 0.3473 | 0.9769 |
| Inhibition Cost | 0.6870 | 0.8411 | 0.9748 | 0.6291 | 0.7631 | 0.5671 |

Rows contain $p$-values corresponding to correlation coefficients in Table 15. Columns represent the signal type including the fixation, neutral, and response-eligible block signals. Lib = liberal, Ali = aligned, Fix = fixation, N = neutral, RE = response-eligible.

### Graph signal alignment and Navon performance covarying for Stroop performance.

Prominent accounts of cognitive control suggest that task switching involves a degree of cognitive inhibition of task sets [13, 14, 15], though the nature of the relationship between cognitive switching and inhibition remains controversial [23, 24, 25]. In the current study, it is important to examine whether the presumed relationship between BOLD signal alignment with underlying neuroanatomy and switching performance is unique among cognitive control measures. To examine this possibility, we used behavioral performance on the Stroop task within subjects as a covariate in partial correlation analyses relating the signal alignment measures with Navon performance. The intuition is that if Navon performance is related to signal alignment when controlling for performance on the Stroop task, then graph signal alignment is related to switching above and beyond basic inhibition. In these analyses, we indeed find that BOLD liberality during all phases of the task remains associated with cognitive switching performance when covarying for performance on the Stroop task within subjects.

Supplementary Table 17: **Pearson's partial correlation coefficients for the relationship between Navon BOLD signal alignment and performance using corresponding Stroop task block performance as a covariate.**

| Behavior | Lib Fix | Lib NS | Lib S | Ali Fix | Ali NS | Ali S |
|---|---|---|---|---|---|---|
| No Switch | 0.2033 | 0.1187 | 0.0596 | 0.2610 | 0.1300 | -0.0341 |
| Switch | 0.2698 | 0.3372 | 0.3146 | 0.2484 | 0.2033 | 0.2494 |
| Switch Cost | 0.5036 | 0.5853 | 0.4590 | 0.3490 | 0.3071 | 0.1546 |

Pearson's correlation coefficients in the Navon task using alignment and liberality values from corresponding blocks and behaviors in the Stroop task and average framewise displacement as covariates. Rows contain partial correlation coefficients associating each median response time at the subject level with their graph liberality. Columns represent the signal type including the fixation, no switch, and switch block signals. Lib = liberal, Ali = aligned, Fix = fixation, NS = no switch, S = switch.

Supplementary Table 18: **Pearson's partial correlation $p$-values for the relationship between Navon BOLD signal alignment and performance using corresponding Stroop task block performance as a covariate.**

| Behavior | Lib Fix | Lib NS | Lib S | Ali Fix | Ali NS | Ali S |
|---|---|---|---|---|---|---|
| No Switch | 0.3296 | 0.5719 | 0.7770 | 0.2076 | 0.5357 | 0.8713 |
| Switch | 0.1921 | 0.0992 | 0.1256 | 0.2313 | 0.3298 | 0.2293 |
| Switch Cost | 0.0103 | 0.0021 | 0.0210 | 0.0873 | 0.1353 | 0.4605 |

Rows contain $p$-values corresponding to correlation coefficients in Table 19. Columns represent the signal type including the fixation, no switch, and switch block signals. Lib = liberal, Ali = aligned, Fix = fixation, NS = no switch, S = switch.

## Graph signal alignment and Navon performance covarying for Stroop BOLD signal alignment.

In addition to covarying for performance on the Stroop inhibition task, we examined whether performance on the Navon task was uniquely related to BOLD signal alignment observed during the Navon task. To test this, we computed partial correlations between Navon task performance and BOLD signal alignment covarying for Stroop signal alignment during the corresponding blocks in the Stroop task (fixation, low control demands, high control demands). This shows us that the relationship between BOLD signal alignment and Navon performance remains significant when covarying for Stroop signal alignment.

Supplementary Table 19: **Pearson's partial correlation coefficients for the association between Navon BOLD signal alignment and behavior using corresponding Stroop task alignment as a covariate.**

| Behavior | Lib Fix | Lib NS | Lib S | Ali Fix | Ali NS | Ali S |
|---|---|---|---|---|---|---|
| No Switch | 0.2502 | 0.2038 | 0.1534 | 0.3362 | 0.2420 | 0.1911 |
| Switch | 0.4530 | 0.4922 | 0.4465 | 0.3817 | 0.3386 | 0.3664 |
| Switch Cost | 0.5785 | 0.6624 | 0.5520 | 0.3682 | 0.3374 | 0.1877 |

Pearson's correlation coefficients assocating Navon task performance with Navon BOLD signal alignment using average framewise displacement and BOLD signal alignments from corresponding blocks in the Stroop task as covariates. Rows contain partial correlation coefficients associating each median response time at the subject level with their graph liberality. Columns represent the signal type including the fixation, no switch, and switch block signals. Lib = Liberal, Ali = Aligned, Fix = fixation, NS = no switch, S = switch.

Supplementary Table 20: **Pearson's partial correlation *p*-values for the association between BOLD signal alignment and behavior using corresponding Stroop task alignment as covariate.**

| Behavior | Lib Fix | Lib NS | Lib S | Ali Fix | Ali NS | Ali S |
|---|---|---|---|---|---|---|
| No Switch | 0.2176 | 0.3180 | 0.4544 | 0.0931 | 0.2336 | 0.3496 |
| Switch | 0.0201 | 0.0106 | 0.0222 | 0.0544 | 0.0906 | 0.0656 |
| Switch Cost | 0.0020 | 0.0002 | 0.0035 | 0.0642 | 0.0919 | 0.3584 |

Rows contain *p*-values corresponding to correlation coefficients in Table 19. Columns represent the signal type including the fixation, no switch, and switch block signals. Lib = liberal, Ali = aligned, Fix = fixation, NS = no switch, S = switch.

### Graph signal alignment in the Stroop fixation correlated with Navon performance.

To examine whether BOLD signal liberality operates like a trait associated with cognitive flexibility *versus* a state, we conducted an analysis relating BOLD liberal signals during the Stroop fixation periods with performance during the Navon. Significant correlations would indicate that BOLD signal liberality in fixation periods in both tasks is associated with Navon switching performance, suggesting that BOLD signal liberality is a trait-like feature associated with cognitive flexibility. Instead, we observe non-significant correlations that suggest that flexibility-associated BOLD liberality is unique to signals observed during the Navon task. This supports the notion that BOLD signal liberality operates like a state under specific task sets associated with cognitive flexibility.

Supplementary Table 21: **Pearson's partial correlation coefficients for the association between Stroop fixation liberality and Navon task performance.**

| Behavior | Stroop Fixation |
|---|---|
| No Switch | -0.0757 |
| Switch | 0.0822 |
| Switch Cost | 0.3016 |

Correlation coefficients for Navon Behavior given Stroop Fixation.

Supplementary Table 22: **Pearson's partial correlation $p$-values for the association between Stroop fixation liberality and Navon task performance.**

| Behavior | Stroop Fixation |
|---|---|
| No Switch | 0.7073 |
| Switch | 0.6835 |
| Switch Cost | 0.1262 |

Correlation $p$-values corresponding to correlation coefficients in Table 21, Navon behavior given stroop fixation.

### Relating interhemispheric liberality and alignment similarity with Navon and Stroop task performance.

Numerous brain functions require coordination across the hemispheres to facilitate cognitive processes. In the context of the current tasks, our global measures of signal alignment and liberality do not explicitly measure the extent to which signal alignment is coordinated across the hemispheres. To explore whether interhemispheric coordination is behaviorally relevant without the graph spectrum analysis framework, we use a measure of interhemispheric similarity in alignment values and associate it with performance. Specifically, after computing the BOLD signal alignment and liberality values, we compute the Pearson's correlation coefficient between homologous pairs across the brain's hemispheres (henceforth "interhemispheric symmetry"). This quantifies the extent to which regions across the brain demonstrate similar signal alignment with their homologue.

We find no relationship between BOLD signal interhemispheric symmetry and performance on the Navon task. However, we find that increased interhemispheric symmetry in liberal signals during response-eligible Stroop blocks is positively associated with inhibition costs. In addition, interhemispheric symmetry in aligned signals during Stroop fixation blocks is negatively associated with response times during each block type. Put differently, mismatching alignment in the most aligned signals across the hemispheres is associated with faster performance, whereas matching liberality across the hemispheres is associated with slower cognitive inhibition. In other words, a double dissociation between switching and inhibition is found in liberal signal properties, where greater alignment in liberal signals facilitates cognitive switch costs, and greater interhemispheric similarity in the same signals is associated with higher inhibition costs. Whereas cognitive switching may benefit from modestly leveraging anatomical network organization, inhibition is more efficient in individuals where the most liberal signals dissociate from one another across the hemispheres. Speculatively, this finding may indicate that failing to rely on similarly anatomically-constrained processing across the hemispheres could diminish information transfer between them, leading to performance decrements on a cognitive inhibition task. We could conduct additional studies to examine whether mechanisms such as interhemispheric inhibition [26] are associated with interhemispheric mismatches in liberality in motor and cognitive inhibition.

Moreover, this exploratory analysis does suggest that BOLD signal alignment differs not only in its relationship to cognition, but also that different ranges of signal alignment contain information about different behavioral properties. In the Stroop task, faster performance associated with the interhemispheric symmetry among the most aligned signals may suggest that separate from inhibition costs *per se*, stability among activity that is strongly organized by underlying anatomy forms a basis for faster responses during simple color-word associations. Whether these signals are relevant to more complex visual and language decoding functions remains to be seen.

Supplementary Table 23: **Pearson's partial correlation coefficients for the association between interhemispheric alignment similarity and Navon task performance using sex, age, and average framewise displacement as covariates.**

| Behavior | Lib Fix | Lib NS | Lib S | Ali Fix | Ali NS | Ali S |
|---|---|---|---|---|---|---|
| No Switch | 0.1026 | 0.3229 | 0.1139 | 0.0074 | -0.2675 | -0.3124 |
| Switch | 0.0259 | 0.2048 | 0.0429 | 0.0006 | -0.2773 | -0.2521 |
| Switch Cost | -0.0996 | -0.0355 | -0.0786 | -0.0102 | -0.2128 | -0.0871 |

Pearson's correlation coefficients in the Navon task using sex, age, and average framewise displacement as a covariate. Rows contain partial correlation coefficients associating each median response time at the subject level with the association of graph signals between hemispheres. Columns represent the signal type including the fixation, no switch, and switch block signals. Lib = interhemispheric similarity of liberal signals between the two hemispheres, Ali = interhemispheric similarity of aligned signals between the two hemispheres, Fix = fixation, NS = no switch, S = switch, WM = working memory.

Supplementary Table 24: **Pearson's partial correlation *p*-values for the association between interhemispheric alignment similarity and Navon task performance using sex, age, and average framewise displacement as covariates.**

| Behavior | Lib Fix | Lib N | Lib RE | Ali Fix | Ali N | Ali RE |
|---|---|---|---|---|---|---|
| No Switch | 0.6735 | 0.1065 | 0.6449 | 0.9562 | 0.1449 | 0.0698 |
| Switch | 0.9859 | 0.3274 | 0.9358 | 0.9793 | 0.1279 | 0.1186 |
| Switch Cost | 0.5494 | 0.8385 | 0.6055 | 0.9801 | 0.2317 | 0.4433 |

Rows contain *p*-values corresponding to correlation coefficients in Table 23. Columns represent the signal type including the fixation, no switch, and switch block signals. Lib = interhemispheric similarity of liberal signals between the two hemispheres, Ali = interhemispheric similarity of aligned signals between the two hemispheres, Fix = fixation, NS = no switch, S = switch.

Supplementary Table 25: **Pearson's partial correlation coefficients for the association between interhemispheric alignment similarity and Stroop task performance using sex, age, and average framewise displacement as covariates.**

| Behavior | Lib Fix | Lib N | Lib RE | Ali Fix | Ali N | Ali RE |
|---|---|---|---|---|---|---|
| Neutral | -0.1495 | -0.4565 | -0.0620 | -0.5912 | -0.3521 | -0.2310 |
| Response-eligible | -0.1450 | -0.3848 | 0.2053 | -0.6039 | -0.3901 | -0.1638 |
| Inhibition Cost | -0.0123 | 0.0863 | 0.5605 | -0.1132 | -0.1320 | 0.1096 |

Pearson's correlation coefficients in during the Stroop task using sex, age, and average framewise displacement as covariates. Rows contain partial correlation coefficients associating each median response time at the subject level with the association of graph signals between hemispheres. Columns represent the signal type including the fixation, no switch, and switch block signals. Lib = interhemispheric similarity of liberal signals between the two hemispheres, Ali = interhemispheric similarity of aligned signals between the two hemispheres, Fix = fixation, N = neutral, RE = response-eligible.

Supplementary Table 26: **Pearson's partial correlation $p$-values for the association between interhemispheric alignment similarity and Stroop task performance using sex, age, and average framewise displacement as covariates.**

| Behavior | Lib Fix | Lib N | Lib RE | Ali Fix | Ali N | Ali RE |
|---|---|---|---|---|---|---|
| Neutral | 0.4757 | 0.0218 | 0.7685 | 0.0019 | 0.0843 | 0.2665 |
| Response-eligible | 0.4891 | 0.0575 | 0.3249 | 0.0014 | 0.0539 | 0.4340 |
| Inhibition Cost | 0.9535 | 0.6815 | 0.0036 | 0.5901 | 0.5293 | 0.6019 |

Rows contain $p$-values corresponding to correlation coefficients in Table 25. Columns represent the signal type including the fixation, no switch, and switch block signals. Lib = interhemispheric similarity of liberal signals between the two hemispheres, Ali = interhemispheric similarity of aligned signals between the two hemispheres, Fix = fixation, N = neutral, RE = response-eligible.

## Aligned and liberal signals in the n-back working memory task.

In the separate sample from the HCP, we examine the associations between median response times in each task condition (0-back, 2-back, and 2-back minus 0-back) to provide a symmetrical analysis to the Navon and Stroop analyses. We replicate these analyses in both the left-to-right and right-to-left phase encoding direction data available through the HCP. In the current data, we find no consistent relationship between signal alignment or liberality with performance measures across the two phase encoding directions. In addition to the prior results, this is consistent with the notion that modest alignment with anatomical networks is associated with cognitive flexibility as opposed to working memory demands. Taken together with our findings in the Stroop, this suggests that the liberality-flexibility relationship is unique among the current cognitive control measures.

Supplementary Table 27: **Pearson's partial correlation coefficients for the association between BOLD signal alignment and the n-back task performance in the left to right phase encoding data.**

| Behavior | Lib Fix | Lib NS | Lib S | Ali Fix | Ali NS | Ali S |
|---|---|---|---|---|---|---|
| 0-back | 0.0379 | 0.0326 | 0.0212 | 0.0504 | -0.0220 | 0.1819 |
| 2-back | -0.0331 | -0.0351 | -0.0524 | 0.0452 | -0.0653 | 0.1251 |
| Difference | -0.1870 | -0.1812 | -0.2080 | 0.0235 | -0.1495 | -0.0309 |

Pearson's correlation coefficients in LR tasks using average framewise displacement, age, and sex as covariates. Rows contain partial correlation coefficients associating each median response time at the subject level with their graph liberality. Columns represent the signal type including the fixation, no switch, and switch block signals. Lib = liberal, Ali = aligned, Fix = fixation, NS = no switch, S = switch.

Supplementary Table 28: **Pearson's partial correlation *p*-values for the association between BOLD signal alignment and the n-back task performance in the left to right phase encoding data.**

| Behavior | Lib Fix | Lib NS | Lib S | Ali Fix | Ali NS | Ali S |
|---|---|---|---|---|---|---|
| 0-back | 0.8288 | 0.8524 | 0.9040 | 0.7736 | 0.9004 | 0.2956 |
| 2-back | 0.8504 | 0.8413 | 0.7650 | 0.7967 | 0.7094 | 0.4739 |
| Difference | 0.2821 | 0.2975 | 0.2306 | 0.8935 | 0.3914 | 0.8600 |

Rows contain $p$-values corresponding to correlation coefficients in Table 27. Columns represent the signal type including the fixation, no switch, and switch block signals. Lib = liberal, Ali = aligned, Fix = fixation, NS = no switch, S = switch.

Supplementary Table 29: **Pearson's partial correlation coefficients for the association between BOLD signal alignment and the n-back task performance in the right to left phase encoding data.**

| Behavior | Lib Fix | Lib NS | Lib S | Ali Fix | Ali NS | Ali S |
|---|---|---|---|---|---|---|
| 0-back | 0.0407 | 0.1804 | 0.1745 | -0.0309 | 0.3005 | 0.2156 |
| 2-back | -0.0432 | 0.0539 | 0.0682 | -0.0749 | 0.2367 | 0.1878 |
| Difference | -0.2279 | -0.2686 | -0.2112 | -0.1525 | -0.0028 | 0.0523 |

Pearson's correlation coefficients in RL tasks using average framewise displacement, age, and sex as covariates. Rows contain partial correlation coefficients associating each median response time at the subject level with their graph liberality. Columns represent the signal type including the fixation, no switch, and switch block signals. Lib = Liberal, Ali = Aligned, Fix = fixation, NS = no switch, S = switch.

Supplementary Table 30: **Pearson's partial correlation $p$-values for the association between BOLD signal alignment and the n-back task performance in the right to left phase encoding data.**

| Behavior | Lib Fix | Lib NS | Lib S | Ali Fix | Ali NS | Ali S |
|---|---|---|---|---|---|---|
| 0-back | 0.8112 | 0.2854 | 0.3016 | 0.8559 | 0.0708 | 0.2000 |
| 2-back | 0.7997 | 0.7515 | 0.6884 | 0.6597 | 0.1584 | 0.2657 |
| Difference | 0.1749 | 0.1080 | 0.2096 | 0.3676 | 0.9870 | 0.7587 |

Rows contain $p$-values corresponding to correlation coefficients in Table 29. Columns represent the signal type including the fixation, no switch, and switch block signals. Lib = liberal, Ali = aligned, Fix = fixation, NS = no switch, S = switch.

## Relating interhemispheric liberality and alignment similarity with Navon and Stroop task performance.

Supplementary Table 31: **Pearson's partial correlation coefficients for interhemispheric alignment similarity during the n-back task using sex, age, and average framewise displacement as covariates.**

| Behavior | Lib Fix | Lib NS | Lib S | Ali Fix | Ali NS | Ali S |
|---|---|---|---|---|---|---|
| No Switch | 0.2585 | 0.0248 | 0.2296 | 0.1573 | -0.1094 | -0.1770 |
| Switch | 0.3241 | 0.0506 | 0.2602 | 0.1749 | -0.1288 | -0.2169 |
| Switch Cost | 0.4025 | 0.0983 | 0.2733 | 0.1768 | -0.1450 | -0.2603 |

Pearson's correlation coefficients in LR tasks using sex, age, and average framewise displacement as covariates. Rows contain partial correlation coefficients associating each median response time at the subject level with the association of graph signals between hemispheres. Columns represent the signal type including the fixation, no switch, and switch block signals. Lib = interhemispheric similarity of liberal signals between the two hemispheres, Ali = interhemispheric similarity of aligned signals between the two hemispheres, Fix = fixation, NS = no switch, S = switch.

Supplementary Table 32: **Pearson's partial correlation $p$-values for interhemispheric alignment similarity during the n-back task using sex, age, and average framewise displacement as covariates.**

| Behavior | Lib Fix | Lib NS | Lib S | Ali Fix | Ali NS | Ali S |
|---|---|---|---|---|---|---|
| No Switch | 0.1337 | 0.8877 | 0.1846 | 0.3668 | 0.5316 | 0.3090 |
| Switch | 0.0575 | 0.7728 | 0.1311 | 0.3151 | 0.4607 | 0.2108 |
| Switch Cost | 0.0165 | 0.5742 | 0.1121 | 0.3097 | 0.4058 | 0.1311 |

Rows contain $p$-values corresponding to correlation coefficients in Table 31. Columns represent the signal type including the fixation, no switch, and switch block signals. Lib = interhemispheric similarity of liberal signals between the two hemispheres, Ali = interhemispheric similarity of aligned signals between the two hemispheres, Fix = fixation, NS = no switch, S = switch.

Supplementary Table 33: **Pearson's partial correlation coefficients for interhemispheric alignment similarity during the n-back task using sex, age, and average framewise displacement as covariates.**

| Behavior | Lib Fix | Lib NS | Lib S | Ali Fix | Ali NS | Ali S |
|---|---|---|---|---|---|---|
| 0-back | -0.2395 | -0.0572 | 0.2025 | -0.0081 | -0.0626 | 0.0120 |
| 2-back | -0.2270 | 0.0002 | 0.2539 | -0.0668 | -0.0517 | 0.0422 |
| Difference | -0.1080 | 0.1346 | 0.2739 | -0.1780 | -0.0058 | 0.0961 |

Pearson's correlation coefficients in RL tasks using sex, age, and average framewise displacement as covariates. Rows contain partial correlation coefficients associating each median response time at the subject level with the association of graph signals between hemispheres. Columns represent the signal type including the fixation, no switch, and switch block signals. Lib = interhemispheric similarity of liberal signals between the two hemispheres, Ali = interhemispheric similarity of aligned signals between the two hemispheres, Fix = fixation, NS = no switch, S = switch.

Supplementary Table 34: **Pearson's partial correlation $p$-values for interhemispheric alignment similarity during the n-back task using sex, age, and average framewise displacement as covariates.**

| Behavior | Lib Fix | Lib NS | Lib S | Ali Fix | Ali NS | Ali S |
|---|---|---|---|---|---|---|
| 0-back | 0.1659 | 0.7439 | 0.2434 | 0.9631 | 0.7209 | 0.9454 |
| 2-back | 0.1898 | 0.9991 | 0.1411 | 0.7028 | 0.7680 | 0.8099 |
| Difference | 0.5370 | 0.4408 | 0.1114 | 0.3064 | 0.9736 | 0.5830 |

Rows contain $p$-values corresponding to correlation coefficients in Table 36. Columns represent the signal type including the fixation, no switch, and switch block signals. Lib = interhemispheric similarity of liberal signals between the two hemispheres, Ali = interhemispheric similarity of aligned signals between the two hemispheres, Fix = fixation, NS = no switch, S = switch.

### The relationship between aligned and liberal signals at rest and n-back working memory task performance.

In the Navon task, we observe that activity across fixation, switching, and non-switching blocks is associated with switching and switch cost response times. Relating the Stroop fixation with the Navon performance yielded an insignificant correlation, suggesting that non-task liberality may represent a facilitative set-specific feature specific cognitive flexibility. Liberality during fixation in the n-back task was also not related to n-back performance. However, we further explored the possibility that non-task BOLD signal alignment may be related to cognitive performance during the n-back. In these analyses, resting state alignment and liberality across the left-to-right and right-to-left phase encoding directions was not significantly associated with n-back performance. This further illustrates that BOLD signal liberality may be a feature of brain network organization facilitating cognitive flexibility specifically under task rule sets including flexibility demands.

Supplementary Table 35: **Pearson's partial correlation coefficients for the relationship between aligned and liberal signals at rest with n-back performance using sex, age, and average framewise displacement as covariates.**

| Behavior | Lib LR | Lib RL | Ali LR | Ali RL |
|---|---|---|---|---|
| 0-back | -0.1218 | -0.1895 | -0.0067 | 0.0303 |
| 2-back | -0.0929 | -0.1951 | -0.0141 | -0.0351 |
| Difference | 0.0006 | -0.1425 | -0.0297 | -0.1809 |

Pearson's correlation coefficients in left to right (LR) and right to left (RL) phase encoding directions for the resting data with n-back performance using sex, age, and average framewise displacement as covariates. Rows contain partial correlation coefficients associating each median response time at the subject level with the graph signals. Columns represent the signal type. Lib = liberal signals, Ali = aligned signals.

Supplementary Table 36: **Pearson's partial correlation *p*-values for the relationship between aligned and liberal signals at rest with n-back performance using sex, age, and average framewise displacement as covariates.**

| Behavior | Lib LR | Lib RL | Ali LR | Ali RL |
|---|---|---|---|---|
| 0-back | 0.5620 | 0.3642 | 0.9746 | 0.8858 |
| 2-back | 0.6589 | 0.3501 | 0.9465 | 0.8678 |
| Difference | 0.9977 | 0.4969 | 0.8879 | 0.3868 |

Rows contain *p*-values for the partial correlation coefficients in Table 36. Columns represent the signal type. Lib = liberal signals, Ali = aligned signals.

## Robustness of aligned and liberal signals to parameter selection

In the main text, we report results where we represent the liberal signals $\mathbf{x}_{\mathrm{L}}$ and aligned signals $\mathbf{x}_{\mathrm{H}}$ using cut points for $K_{\mathrm{L}}$ and $K_{\mathrm{H}}$ of the ten lowest (of $K_{\mathrm{L}}$) and highest ($K_{\mathrm{H}}$) values. To test the robustness of aligned and liberal signals to variations in these parameters, we decompose the observed BOLD signals during the Navon task into $\mathbf{x}_{\mathrm{L}}$ and $\mathbf{x}_{\mathrm{H}}$ under the choice of $K_{\mathrm{L}}$ and $K_{\mathrm{H}}$ from five below to five above the choice of parameters studied in the main manuscript. We then compute the correlation coefficient among $\mathbf{x}_{\mathrm{L}}$ and $\mathbf{x}_{\mathrm{H}}$ across all TRs for all subjects to examine the stability of aligned and liberal signals. We find that the observed signal decomposition is stable across parameter choices: for $\mathbf{x}_{\mathrm{L}}$ (liberal signals), the values are correlated at a mean of $R = 0.95$ (St.D. 0.03); for $\mathbf{x}_{\mathrm{H}}$ (aligned signals), the values are correlated at a mean of $R = 0.99$ (St.D. 0.02). Thus, the signals examined in the main text are highly stable over the choice of definition for the range of aligned and liberal signals, and especially for liberal signals.

## Null permutation test for the significance of the anatomical organization of signals

In the current analysis, the aligned signals are found to be the most concentrated in systems including those known to be functionally flexible in prior studies [1, 2]. It is interesting to establish whether system signal organization is driven by simple spatial correlations in the data *versus* more complex features of network organization. To test whether these concentrated signals are driven by spatial correlations in aligned and liberal signals among pairs of regions, we calculated the Euclidean distance between the mean voxel coordinates for each region of interest. Then, we calculated the original similarity between pairs of regions as the arithmetic difference between the aligned or liberal signals observed in each region. Finally, we computed the Pearsons correlation between the region distances and signal similarity. Notably, we find no spatial correlation between aligned ($R = 0.00, p = 1.0$; below machine precision) or liberal ($R = 0.00$, $p = 1.0$; below machine precision) signals in the current data. This indicates that the signal embedding observed in systems is not driven by simple spatial relationships among regions.

Thus, it is further interesting to examine the complexity of anatomical network contributions to these signals. We consider whether anatomically aligned signals are organized by the simple contributions of nearest neighbor nodes in anatomical networks (i.e., only the nodes that share direct connections to each node) *versus* the specific configuration of the entire anatomical network. This allows us to identify whether the BOLD signals inclusive of the most flexible systems in the brain are aligned with anatomy as a function of the contribution of the entire network, which would potentially suggest that functionally flexible systems are organized by weighted contributions from the entire brain.

To test this possibility, we conduct a non-parametric permutation test. Specifically, we randomize each individual's network 2000 times preserving the strength and degree sequence of nodes in the network. Then, we decompose the observed BOLD value for each region into its corresponding node in the randomized network across all TRs. We then calculate over subjects the average variance in original BOLD signals accounted for by the eigenvectors associated with the aligned signals for each random permutation. We summarize these values as the mean variance accounted for across all null permutations and compare it to the mean variance accounted for by the original anatomical networks. We observe that the variance accounted for in the real networks exceeds that accounted for in 100% of the null permutations. This indicates that the BOLD signals are organized by anatomical features at a greater topological length across the networks than the direct connections among nodes (See Fig. 4). This finding indicates that signals that depend on underlying anatomy represent complex contributions from anatomical network topology.

The behavioral relevance of this anatomically-aligned organization may be established in future studies. In particular, when the underlying network is constructed from fMRI measurements (functional similarity networks constructed from correlations), it is known that the components of BOLD signals that are the most aligned to the network also explain the most variation across time [11]. Here also we find that signals aligned with anatomical connectivity contain BOLD measurements that are the most variable over time in cingulo-opercular and fronto-parietal systems. Functional connectivity (e.g., correlation, coherence, and mutual information) networks evince similar but not completely overlapping topology when compared to anatomical networks [27]. Thus, analyzing the alignment of measured correlations on anatomical networks may provide an important extension to understand signals in the time domain in the human connectome. Mathematically, the same phenomenon for functional as well as anatomical networks implies that the eigenspectrum of the anatomical network is not that different from functional connectivity. Speculatively, this could provide a meaningful and efficient method to reliably recover anatomical networks from functional connectivity networks.

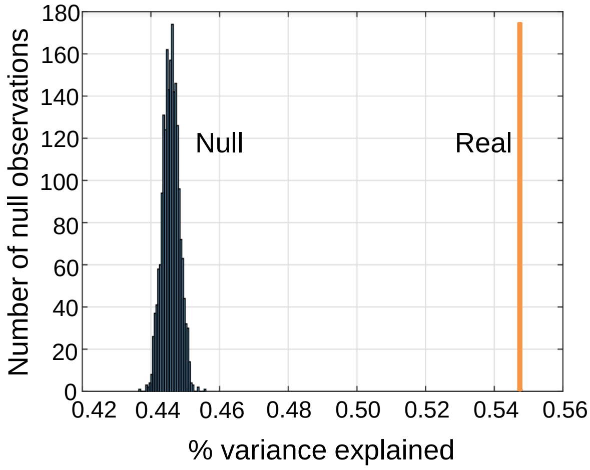


Supplementary Figure 3: **Aligned signals are organized by topologically distant anatomical organization.** We conducted null permutation test with the networks from the 28 subjects. Left: in the null permutations where the edges of the anatomical networks were randomized, a mean of 0.455% variance is accounted for by the eigenvectors corresponding to the aligned parts of the signal. In the observed data, a mean of 0.547% of variance is accounted for by the anatomical networks in their true configurations.

## Alternate measures of function and anatomy

Do anatomy-decomposed functional BOLD signals better related to switch costs than other measures with similar intuitions? To test this possibility, we consider four comparison analyses involving the subcortical system from which the behaviorally relevant signals in our primary analyses originated. First, we compute the mean BOLD signal variance over all subcortical regions for each TR. This correlation represents a measure of differences in BOLD signals at each time measurement without considering its anatomical network context. We then relate the average BOLD signal variance over TRs to switch costs and find no significant relationship ($R = -0.09$, $p = 0.68$). Second, we compute the mean node *strength* – the sum of connections to the node – for each region in the subcortical system. This represents the overall influence of the subcortical regions in the broader anatomical network. We calculate the Pearson correlation coefficient between the mean subcortical node strength and switch costs across subjects, and we find no significant relationship ($R = -0.15$, $p = 0.48$). Third, as a simple measure of the relationship between anatomical and functional connectivity, we computed functional connectivity as the correlations among each regional pair of BOLD time series in each block type correlated this value with anatomical connectivity between each regional pair. Then, we correlated this coefficient with switch costs across subjects, finding no significant relationship for any block type (fixation: $R = 0.05$, $p = 0.7975$; no switch: $R = 0.07$, $p = 0.7338$; switch: $R = -0.23$, $p = 0.24$). Finally, within each subject, we compute the mean Pearson correlation coefficient between each BOLD signal TR and node strengths within the subcortical system, then we compute the Pearson correlation coefficient between these values and switch costs across subjects, finding no significant relationship ($R = 0.17$, $p = 0.41$). Taken together, these results demonstrate that simple measures of BOLD variation, local anatomical network influences, and the relationship between the two are insufficient to account for switch cost variability over subjects. Indeed, decomposing signals in the context of the entire anatomical network provides superior associative value for the cognitive control measure.

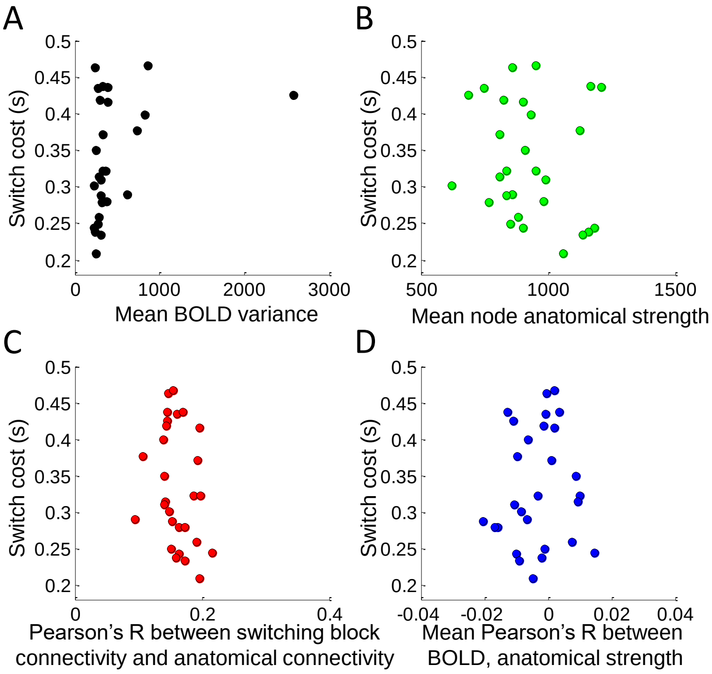


Supplementary Figure 4: **Alternate measures of framewise BOLD variance, anatomy, and function-anatomy relationships in subcortical systems do not associate with switch costs.** We computed alternate function-anatomy measures for each of the 28 subjects and associated them with performance. *(A)* The relationship between mean BOLD variance in the subcortical system and switch costs. *(B)* The relationship between mean anatomical node degree in the subcortical system and switch costs. *(C)* The relationship between Pearson's correlation coefficients between all anatomical and functional connections and switch costs across subjects. *(D)* The relationship between the correlation between BOLD signals and anatomical node degree across regions in the subcortical systems and switch costs.

## Anatomical network null model for behavioral correlations with switch costs.

To examine the importance of the specific anatomical configuration of brain networks for the association between liberal signals and switch costs, we performed a null permutation test. Specifically, we performed 200 permutations in which we generated a random network preserving the strength and degree distributions of the original anatomical networks for each subject. Then, we repeated the BOLD signal decomposition into the null anatomical network for each subject and correlated the liberal signals with switch costs in each permutation to generate a null distribution of correlations. From this null distribution, we computed the proportion of null correlation values greater than the observed correlation when using the real anatomical networks. We find that the observed correlation is greater than 99% of correlations (Fig. 8). This result indicates that the specific configuration of the true anatomical network drives the correlation between liberal signal alignment and switch costs.

## Relationships between motion and signal alignment.

In the results reported in the main text and supplement, we included a motion covariate (average framewise displacement across BOLD TRs) in all analyses. Motion is not significantly correlated with switch cost ($R = 0.26$, $p = 0.16$), but is correlated significantly with liberal signals ($R = 0.77$, $p = 1.10 \times 10^{-6}$), justifying its inclusion as a covariate in behavioral analyses. Importantly, when motion is not included as a covariate in the partial correlation between liberal signals and switch costs, the correlation ($R = 0.59$ , $p = 0.001$) is highly similar to that observed when including motion as a covariate ($R = 0.57$, $p = 0.002$). This finding indicates that the behaviorally relevant portion of the liberal signals is not driven by motion.

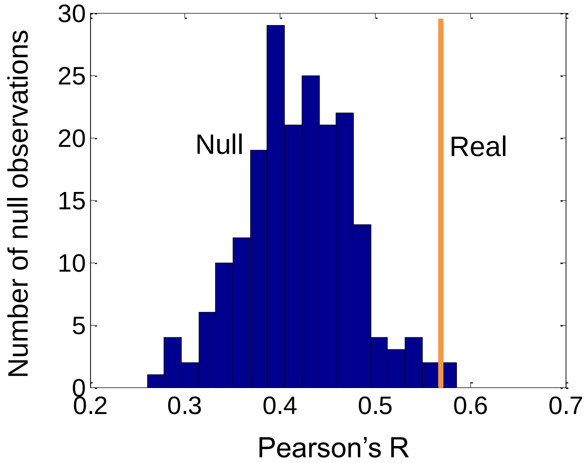


Supplementary Figure 5: **A null permutation test demonstrates that specific anatomical network organization is required to identify behaviorally relevant BOLD signals.** Blue bars in the histogram illustrate the Pearson's correlation coefficients between switch costs and liberal signals over null permutations computed using the 28 subjects' network data. Orange line designates the observed correlation value of the real network.

## General linear model results

In the main text, we examine BOLD signal alignment in the brain. To examine whether our Navon switching task exhibits similar BOLD contrast effects to previous cognitive switching tasks, we performed a traditional general linear model analysis on our BOLD data in FSL [28]. First, we computed the contrast for no-switching blocks > fixation blocks. Then, we computed the contrast for switching blocks > fixation. Finally, comparing the switch > no switch blocks for all subjects in MNI space. This last contrast reveals bilateral frontal, basal ganglia, parietal, and cerebellar activation frequently observed in switching tasks (cf. [29]). Here, we report the region peaks and estimated regions using an MNI to Talairach space conversion in GingerALE [30, 31] and peak coordinate anatomical location estimates from the Talairach client [32].

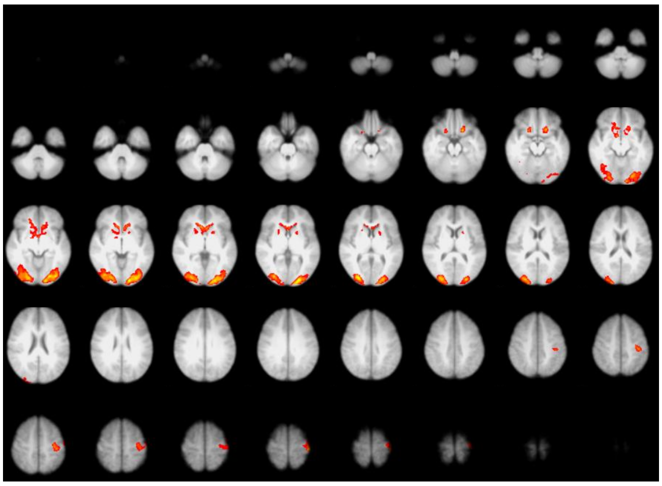

Supplementary Figure 6: **Activation for the contrast Navon no-switch blocks > fixation blocks using the general linear model.** For the 28 subjects, results are presented in radiological convention (Left and right flipped). The contrast represents the cluster-corrected z-score map at a threshold of $z > 2.3$, $p < 0.05$.

Supplementary Table 37: MNI coordinates for the no-swtich > fixation contrast and regions estimated using the Talairach space conversion.

| Voxels | Z-score | X | Y | Z | Hemisphere | Region | Area |
|---|---|---|---|---|---|---|---|
| 5 | 5.14 | -22 | -93.6 | 3.6 | Left Cerebrum | Middle Occipital Gyrus | Brodmann area 18 |
| 4 | 5.26 | -15.5 | -93.5 | -5.49 | Left Cerebrum | Lingual Gyrus | Brodmann area 17 |
| 1 | 5.11 | -24 | -84 | -8 | Left Cerebrum | Middle Occipital Gyrus | Brodmann area 18 |

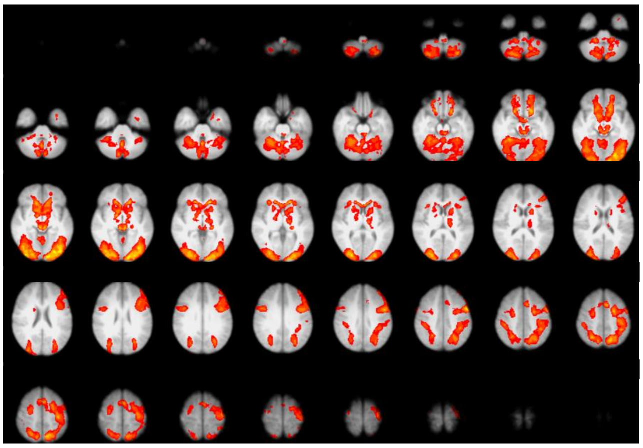

Supplementary Figure 7: **Activation for the contrast Navon switching blocks > fixation blocks using the general linear model.** For the 28 subjects, results are presented in radiological convention (Left and right flipped). The contrast represents the cluster-corrected z-score map at a threshold of $z > 2.3$, $p < 0.05$.

Supplementary Table 38: MNI coordinates for the switch > fixation contrast and regions estimated using the Talairach space conversion.

| Voxels | Z-score | X | Y | Z | Hemisphere | Region | Area |
|---|---|---|---|---|---|---|---|
| 528 | 6.39 | -26.5 | -87.5 | -5.23 | Left Cerebrum | Inferior Occipital Gyrus | Brodmann area 18 |
| 134 | 5.84 | 30.5 | -88.7 | -4.27 | Right Cerebrum | Inferior Occipital Gyrus | Brodmann area 18 |
| 31 | 5.61 | -12.7 | -65.7 | 54.5 | Left Cerebrum | Superior Parietal Lobule | Brodmann area 7 |
| 31 | 5.7 | 27.4 | -90.2 | 9.23 | Right Cerebrum | Middle Occipital Gyrus | Brodmann area 18 |
| 21 | 5.37 | -16.8 | 18.9 | -15.9 | Left Cerebrum | Inferior Frontal Gyrus | Brodmann area 47 |
| 19 | 5.77 | -51.1 | 4.52 | 42.5 | Left Cerebrum | Middle Frontal Gyrus | Brodmann area 6 |
| 9 | 5.68 | -4.47 | -30.2 | -3.96 | Left Cerebrum | Thalamus | Pulvinar |
| 7 | 5.18 | 44 | -71.7 | -9.72 | Right Cerebrum | Fusiform Gyrus | Brodmann area 19 |
| 5 | 5.21 | 12.4 | 25.6 | -9.2 | Right Cerebrum | Medial Frontal Gyrus | Brodmann area 11 |
| 4 | 5.36 | 5.51 | -29 | -4.49 | Right Cerebrum | Thalamus | * |
| 3 | 5.08 | 32 | -45.3 | -17.3 | Right Cerebellum | Culmen | * |
| 1 | 5.03 | -36 | -22 | 56 | Left Cerebrum | Precentral Gyrus | Brodmann area 4 |
| 1 | 5.28 | -8 | 14 | 52 | Left Cerebrum | Superior Frontal Gyrus | Brodmann area 6 |
| 1 | 5.01 | -24 | -2 | 50 | Left Cerebrum | Middle Frontal Gyrus | Brodmann area 6 |
| 1 | 5 | 26 | -82 | -6 | Right Cerebrum | Middle Occipital Gyrus | Brodmann area 18 |
| 1 | 5.02 | -12 | 28 | -10 | Left Cerebrum | Anterior Cingulate | Brodmann area 32 |
| 1 | 5.03 | 20 | 18 | -16 | Right Cerebrum | Inferior Frontal Gyrus | Brodmann area 47 |
| 1 | 5.03 | 2 | -56 | -34 | Right Cerebellum | Cerebellar Tonsil | * |

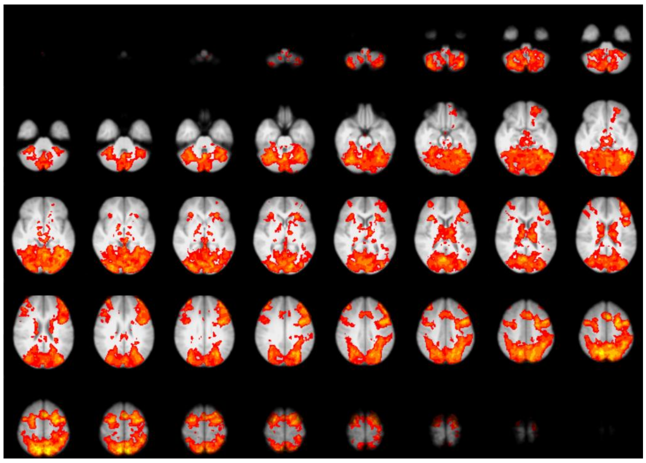

Supplementary Figure 8: **Activation for the contrast Navon switch > no switch blocks using the general linear model.** For the 28 subjects, results are presented in radiological convention (Left and right flipped). The contrast represents the cluster-corrected z-score map at a threshold of $z > 2.3$, $p < 0.05$.

Supplementary Table 39: **MNI coordinates for the switching > no switching contrast and regions estimated using the Talairach space conversion.**

| Voxels | Z-score | X | Y | Z | Hemisphere | Region | Area |
|---|---|---|---|---|---|---|---|
| 294 | 6.23 | 10.68 | -66.11 | 48.61 | Right Cerebrum | Precuneus | Brodmann area 7 |
| 246 | 6.15 | -12.42 | -68.14 | 47.61 | Left Cerebrum | Precuneus | Brodmann area 7 |
| 117 | 5.72 | -26.29 | -2.78 | 52.32 | Left Cerebrum | Sub-Gyral | Brodmann area 6 |
| 80 | 5.68 | -40.07 | 0.78 | 43.51 | Left Cerebrum | Middle Frontal Gyrus | Brodmann area 6 |
| 65 | 5.46 | -37.78 | -59.61 | -10.53 | Left Cerebrum | Fusiform Gyrus | Brodmann area 37 |
| 34 | 5.44 | -3.39 | 8.28 | 54.09 | Left Cerebrum | Superior Frontal Gyrus | Brodmann area 6 |
| 32 | 5.63 | 23.95 | -4.39 | 59.49 | Right Cerebrum | Middle Frontal Gyrus | Brodmann area 6 |
| 23 | 5.5 | -7.81 | -52.9 | 49.9 | Left Cerebrum | Precuneus | Brodmann area 7 |
| 22 | 5.91 | 2.58 | -69.62 | 11.05 | Right Cerebrum | Cuneus | Brodmann area 30 |
| 18 | 5.29 | -28.92 | -44.92 | -15.13 | Left Cerebellum | Culmen | * |
| 17 | 5.72 | -38.17 | -44.32 | 50.72 | Left Cerebrum | Inferior Parietal Lobule | Brodmann area 40 |
| 16 | 5.64 | -28.58 | 0.54 | 65.55 | Left Cerebrum | Superior Frontal Gyrus | Brodmann area 6 |
| 15 | 5.37 | -14.62 | -83.3 | 1.01 | Left Cerebrum | Lingual Gyrus | Brodmann area 17 |
| 11 | 5.33 | -38 | -51.49 | 45.28 | Left Cerebrum | Inferior Parietal Lobule | Brodmann area 40 |
| 9 | 5.13 | -27.88 | -65.49 | 29.23 | Left Cerebrum | Precuneus | Brodmann area 7 |
| 8 | 5.35 | -34.52 | -76.13 | 20.9 | Left Cerebrum | Middle Temporal Gyrus | Brodmann area 19 |
| 7 | 5.23 | 22.94 | -53.94 | 48.75 | Right Cerebrum | Precuneus | Brodmann area 7 |
| 5 | 5.25 | -19.55 | -65.37 | 29.29 | Left Cerebrum | Precuneus | Brodmann area 7 |
| 5 | 5.29 | -0.03 | -52.21 | -29.81 | Right Cerebellum | Nodule | * |
| 4 | 5.25 | -21.57 | 5.79 | 70.01 | Left Cerebrum | Superior Frontal Gyrus | Brodmann area 6 |
| 4 | 5.27 | 9.53 | -72.38 | 8.56 | Right Cerebrum | Cuneus | Brodmann area 23 |
| 4 | 5.14 | -7.04 | -87.36 | -7.9 | Left Cerebrum | Lingual Gyrus | Brodmann area 18 |
| 4 | 5.3 | 35.68 | -63.46 | -22.36 | Right Cerebellum | Declive | * |
| 3 | 5.15 | -12.57 | 2.13 | 64.21 | Left Cerebrum | Medial Frontal Gyrus | Brodmann area 6 |
| 3 | 5.27 | -28.56 | -64.67 | 38.69 | Left Cerebrum | Precuneus | Brodmann area 7 |
| 2 | 5.09 | -33.59 | -54.58 | 55.6 | Left Cerebrum | Superior Parietal Lobule | Brodmann area 7 |
| 2 | 5.14 | 7.1 | -57.66 | 53.84 | Right Cerebrum | Precuneus | Brodmann area 7 |
| 2 | 5.11 | -41.79 | 5.64 | 23.28 | Left Cerebrum | Inferior Frontal Gyrus | Brodmann area 9 |
| 2 | 5.43 | -35 | 50.31 | 23.51 | Left Cerebrum | Superior Frontal Gyrus | Brodmann area 10 |
| 2 | 5.14 | 13.79 | -69.5 | 15.11 | Right Cerebrum | Cuneus | Brodmann area 18 |
| 2 | 5.06 | -4.12 | -62.38 | -4.44 | Left Cerebellum | Culmen of Vermis | * |
| 2 | 5.22 | -4.09 | -59.3 | -7.86 | Left Cerebellum | Culmen | * |
| 2 | 5.13 | 28.12 | -58.66 | -22.1 | Right Cerebellum | Culmen | * |
| 2 | 5.04 | -28.65 | -56.15 | -24.09 | Left Cerebellum | Culmen | * |
| 1 | 5.01 | -23.96 | -8.21 | 58.68 | Left Cerebrum | Middle Frontal Gyrus | Brodmann area 6 |
| 1 | 5.01 | -27.94 | -66.6 | 49.42 | Left Cerebrum | Superior Parietal Lobule | Brodmann area 7 |
| 1 | 5.04 | -20.31 | -58.39 | 39.15 | Left Cerebrum | Precuneus | Brodmann area 7 |
| 1 | 5.08 | -44.62 | 21.68 | 40.59 | Left Cerebrum | Middle Frontal Gyrus | Brodmann area 8 |
| 1 | 5.12 | 28.89 | -67.95 | 33.4 | Right Cerebrum | Precuneus | Brodmann area 7 |
| 1 | 5.03 | -29.8 | -71.11 | 31.02 | Left Cerebrum | Precuneus | Brodmann area 19 |
| 1 | 5.16 | 33.09 | 44.22 | 35.3 | Right Cerebrum | Middle Frontal Gyrus | Brodmann area 9 |
| 1 | 5.02 | -20.29 | -65.04 | 24.24 | Left Cerebrum | Precuneus | Brodmann area 31 |
| 1 | 5.07 | -10.86 | -84.94 | 6.72 | Left Cerebrum | Cuneus | Brodmann area 17 |
| 1 | 5.12 | 27.02 | -90.03 | -7.86 | Right Cerebrum | Inferior Occipital Gyrus | Brodmann area 18 |
| 1 | 5.03 | -31.5 | -47.69 | -7.27 | Left Cerebrum | Fusiform Gyrus | Brodmann area 37 |
| 1 | 5.11 | -33.33 | -60.29 | -47.92 | Left Cerebellum | Cerebellar Tonsil | * |

## References


[1] Mattar, M. G., Betzel, R. F. & Bassett, D. S. The flexible brain. *Brain* **139**, 2110–2112 (2016).

[2] Braun, U. *et al.* Dynamic reconfiguration of frontal brain networks during executive cognition in humans. *Proceedings of the National Academy of Sciences* **112**, 11678–11683 (2015).

[3] Bassett, D. S. *et al.* Robust detection of dynamic community structure in networks. *Chaos: An Interdisciplinary Journal of Nonlinear Science* **23**, 013142 (2013).

[4] Bassett, D. S. *et al.* Dynamic reconfiguration of human brain networks during learning. *Proceedings of the National Academy of Sciences* **108**, 7641–7646 (2011).

[5] Mucha, P. J., Richardson, T., Macon, K., Porter, M. A. & Onnela, J.-P. Community structure in time-dependent, multiscale, and multiplex networks. *Science* **328**, 876–878 (2010).

[6] Bassett, D. S. & Siebenhühner, F. Multiscale network organization in the human brain. *Multiscale Analysis and Nonlinear Dynamics: From Genes to the Brain* 179–204 (2013).

[7] Leonardi, N. *et al.* Principal components of functional connectivity: a new approach to study dynamic brain connectivity during rest. *NeuroImage* **83**, 937–950 (2013).

[8] Viviani, R., Grön, G. & Spitzer, M. Functional principal component analysis of fmri data. *Human brain mapping* **24**, 109–129 (2005).

[9] Sandryhaila, A. & Moura, J. M. Discrete signal processing on graphs. *IEEE transactions on signal processing* **61**, 1644–1656 (2013).

[10] Ma, J., Huang, W., Segarra, S. & Ribeiro, A. Diffusion filtering for graph signals and its use in recommendation systems. In *Acoustics, Speech and Signal Processing (ICASSP), 2016 IEEE Int. Conf. on*, 4563–4567 (Shanghai, China, 2016).

[11] Huang, W. *et al.* Graph frequency analysis of brain signals. *J. Sel. Topics Signal Process.* **10**, 1189–1203 (2016).

[12] Miyake, A. *et al.* The unity and diversity of executive functions and their contributions to complex frontal lobe tasks: A latent variable analysis. *Cognitive psychology* **41**, 49–100 (2000).

[13] Norman, D. & Shallice, T. Attention to action (pp. 1-18). *US: Springer* (1986).

[14] Diamond, A. Normal development of prefrontal cortex from birth to young adulthood: Cognitive functions, anatomy, and biochemistry. *Principles of frontal lobe function* 466–503 (2002).

[15] Davidson, M. C., Amso, D., Anderson, L. C. & Diamond, A. Development of cognitive control and executive functions from 4 to 13 years: Evidence from manipulations of memory, inhibition, and task switching. *Neuropsychologia* **44**, 2037–2078 (2006).

[16] Duncan, J., Schramm, M., Thompson, R. & Dumontheil, I. Task rules, working memory, and fluid intelligence. *Psychonomic bulletin & review* **19**, 864–870 (2012).

[17] Van Essen, D. C. *et al.* The wu-minn human connectome project: an overview. *Neuroimage* **80**, 62–79 (2013).

[18] Ciric, R. *et al.* Benchmarking of participant-level confound regression strategies for the control of motion artifact in studies of functional connectivity. *Neuroimage* (2017).

[19] Stroop, J. R. Studies of interference in serial verbal reactions. *Journal of experimental psychology* **18**, 643 (1935).

[20] January, D., Trueswell, J. C. & Thompson-Schill, S. L. Co-localization of stroop and syntactic ambiguity resolution in broca's area: Implications for the neural basis of sentence processing. *Journal of Cognitive Neuroscience* **21**, 2434–2444 (2009).

[21] West, R. & Alain, C. Age-related decline in inhibitory control contributes to the increased stroop effect observed in older adults. *Psychophysiology* **37**, 179–189 (2000).

[22] Kane, M. J., Conway, A. R., Miura, T. K. & Colflesh, G. J. Working memory, attention control, and the n-back task: a question of construct validity. *Journal of Experimental Psychology: Learning, Memory, and Cognition* **33**, 615 (2007).

[23] Koch, I., Gade, M., Schuch, S. & Philipp, A. M. The role of inhibition in task switching: A review. *Psychonomic bulletin & review* **17**, 1–14 (2010).

[24] de Bruin, A., Roelofs, A., Dijkstra, T. & FitzPatrick, I. Domain-general inhibition areas of the brain are involved in language switching: Fmri evidence from trilingual speakers. *NeuroImage* **90**, 348–359 (2014).

[25] Gade, M., Schuch, S., Druey, M. D. & Koch, I. Inhibitory control in task switching. *Task Switching and Cognitive Control* 137–159 (2014).

[26] Ferbert, A. *et al.* Interhemispheric inhibition of the human motor cortex. *The Journal of physiology* **453**, 525–546 (1992).

[27] Bullmore, E. & Sporns, O. Complex brain networks: graph theoretical analysis of structural and functional systems. *Nature Reviews Neuroscience* **10**, 186–198 (2009).

[28] Jenkinson, M., Beckmann, C. F., Behrens, T. E., Woolrich, M. W. & Smith, S. M. Fsl. *Neuroimage* **62**, 782–790 (2012).

[29] Wager, T. D., Jonides, J. & Reading, S. Neuroimaging studies of shifting attention: a meta-analysis. *Neuroimage* **22**, 1679–1693 (2004).

[30] Lancaster, J. L. *et al.* Bias between mni and talairach coordinates analyzed using the icbm-152 brain template. *Human brain mapping* **28**, 1194–1205 (2007).

[31] Turkeltaub, P. E., Eden, G. F., Jones, K. M. & Zeffiro, T. A. Meta-analysis of the functional neuroanatomy of single-word reading: method and validation. *Neuroimage* **16**, 765–780 (2002).

[32] Lancaster, J., Summerln, J., Rainey, L., Freitas, C. & Fox, P. The talairach daemon, a database server for talairach atlas labels. *Neuroimage* **5**, S633 (1997).